Antimony quartz and antimony-gold quartz veins from northern Portugal

A.M.R. Neiva, P. Andráš, J.M.F. Ramos

PII: S0169-1368(08)00055-3
DOI: doi: 10.1016/j.oregeorev.2008.03.004
Reference: OREGEO 714

To appear in: *Ore Geology Reviews*

Received date: 10 August 2006
Accepted date: 16 March 2008

Please cite this article as: Neiva, A.M.R., Andráš, P., Ramos, J.M.F., Antimony quartz and antimony-gold quartz veins from northern Portugal, *Ore Geology Reviews* (2008), doi: 10.1016/j.oregeorev.2008.03.004

Antimony quartz and antimony-gold quartz veins from northern Portugal

A.M.R. Neiva[1*], P. Andráš[2], J.M.F. Ramos[3]

[1] *Department of Earth Sciences, University of Coimbra, 3000-272 Coimbra, Portugal*

[2] *Geological Institute, Slovak Academy of Sciences, Severnás, 97401 Banská Bystrica, Slovakia and Department of Environmental Management, Faculty of Natural Sciences, Matej Bel University, Tajovského 40, 974 01 Banská Bystrica, Slovakia*

[3] *Laboratory of Mining and Geological Institute, 4466-956 S. Mamede de Infesta, Portugal*

Received 10 August 2006; accepted 16 March 2008

Abstract

Antimony- and Pb-Sb-quartz veins from the Bragança district, Portugal, are mainly hosted by Silurian phyllites. Antimony-Au-quartz veins from the Dúrico-Beirã region are mainly hosted by a Cambrian schist-metagraywacke complex, as well as Ordovician phyllites and quartzites. The deposits were mostly exploited in the late 19th Century. Mineralogical characteristics and chemical compositions of individual ore minerals are similar in the two areas. First and second generations of arsenopyrite precipitated at 390 and 300ºC, respectively. Berthierite and stibnite are the most abundant Sb-bearing minerals and precipitated between 225 and 128ºC, native antimony at <200ºC. Drastic fluid cooling is the main cause of mineral precipitation. The Pb isotope compositions of stibnite suggest a homogeneous crustal source of lead, from the metasedimentary sequences, for Sb, Pb-Sb and Sb-Au deposits in both areas, which is consistent with the findings for comparable mineralizations elsewhere in Europe. Remobilization of Pb is related to Variscan metamorphism and deformation.

* Fax: +351-239860501; E-mail address: neiva@dct.uc.pt

Keywords: Antimony, lead-antimony, antimony-gold deposits, ore mineral compositions, ore genesis, Bragança, Dúrico-Beirã, Portugal, stibnite, berthierite.

1. Introduction

Antimony-gold quartz veins occur in terranes dominated by metasedimentary sequences, for example in Alaska (Goldfarb et al., 1993), Australia (e.g., O'Shea and Pertzel, 1988; Huston et al., 2002), Bolivia (Dill et al., 1995), Canada (e.g., Kontak et al., 1996), China (Hutchinson, 1983), Europe (e.g., Gokce and Spiro, 1994; Dill, 1998; Wagner and Cook, 2000; Wagner and Schneider, 2002), and New Zealand (e.g., Pitcairn et al., 2006). Others occur in Archean cratons, for example in Africa (e.g., Buchholz et al., 2007) and Australia (e.g., Hagemann and Lüders, 2003).

The Iberian Massif is the southwestern extension of the European Variscan Belt and one of the largest domains of the Variscan orogen. In the Iberian Massif, most antimony deposits, some of them gold-bearing, occur in the Central Iberian Zone (Gumiel and Arribas, 1987). They are mainly hosted by Cambrian metasedimentary rocks and outcrop within the cores of Variscan anticlines. These mineralized veins are genetically related to granitic rocks (Gumiel, 1983; Ortega et al., 1996) or are due to dilution (fluid mixing) of CO_2-rich metamorphic fluids by surface-derived H_2O-NaCl fluids (Couto et al., 1990). In the German part of the Variscan orogenic belt, this vein mineralization is related to the influx of deep-sourced fluids during late-orogenic exhumation (Wagner and Cook, 2000); ore lead had been extracted from Paleozoic sedimentary sequences (Wagner and Schneider, 2002).

In northern Portugal, Sb- and Pb-Sb-quartz veins occur in the Bragança district (Fig. 1) and Sb-Au quartz veins in the Dúrico-Beirã region (Fig. 2). They were mostly exploited in the late 19th

Century (e.g., Carvalho, 1981). However, in the Bragança district, at Canedo, Serrinha and Sítio da Coitadinha (Fig. 1), exploitation took place from 1943 to 1945 and at Cabeço da Mina, ores were mined from 1952 to 1955. About 33 t of antimony were produced in the Bragança district from 8 mines. At the end of the 19th Century, there were 63 registered antimony areas in the Dúrico-Beirã region, some of the deposits also contained gold. The twelve main mines from this region produced about 12,000 t of high-grade antimony ore containing 2 t of gold (Carvalho, 1981). Some of the veins have been studied previously, notably the Pb-Sb-quartz veins (Neiva, 1956; Noronha et al., 1998) and some Sb-Au-quartz veins (Portugal Ferreira et al., 1971; Santarém Andrade and Portugal Ferreira, 1976; Couto et al., 1990; Couto, 1995).

The present contribution gives a review of various historically important Sb-, Pb-Sb and Sb-Au deposits in northern Portugal, and provides a summary of their key mineralogical features. We also give new mineralogical and Pb-isotope data indicating a single source for all deposits.

2. Geological setting

The Iberian massif has been divided into five tectonostratigraphic zones running parallel to the Variscan fold axes. In the context of the European Variscan foldbelt, these zones generally show great lateral continuity (e.g., Gibbons and Moreno, 2002). The Bragança district is mainly within the Galiza and Trás-os-Montes Zone and the Dúrico-Beirã region lies within the Central Iberian Zone (Fig. 1a). In this zone, deposition of the Carboniferous succession was mainly coeval with the Variscan deformation, when the whole Palaeozoic Gondwanan shelf sequence was deformed and metamorphosed during collision between Gondwana and Laurentia (Gibbons and Moreno, 2002).

2.1 Bragança district

The Bragança district consists of four allochthonous thrust sheets (Fig. 1b, c) on top of the Lower Cambrian to probable Lower Devonian authochton (Ribeiro et al., 1990). Lower and Middle Cambrian phyllites, alternating with metagraywackes, and local metaconglomerates to metasandstones with metavolcanic intercalations, are followed by Lower and probably Middle Ordovician metaconglomerates, quartzites and phyllites. These are overlain by upper Llanvirnian-Landeillian black slates, metagraywackes and a volcanic metasedimentary complex formed by hematitic phyllites and quartzites with intercalations of marbles and basic metavolcanics. The Silurian is represented by metatillites, graphitic phyllites, metalydites, calc-schists and metatuff. The Lower Devonian consists of metatuff, quartzites and the Upper Devonian is represented by metaconglomerates and -tuff (Ribeiro, 1974; Serviços Geológicos de Portugal, 1992). Variscan folding and overthrusting took place in the area (Ribeiro et al., 1990).

In the Bragança district, there are several Sb-quartz veins and some Pb-Sb-quartz veins with lenticular structures, which are 100 m to 200 m long, up to 1.3 m thick and contain sulfides and sulfosalts, (Fig. 1c, Table 1). Most of these veins fill faults that intersect the lower allochthonous thrust complex. The antimony ores, however, are only found when hydrothermal precipitation has taken place in Silurian phyllites (Table 1). These veins have a brecciated structure, containing fragments of quartz and phyllite, locally of metagraywacke and quartzite, cemented by quartz aggregates, which also contain secondary muscovite and, locally, barite, ankerite and calcite. The characteristics of these veins are summarized in Table 1.

2.2 Dúrico-Beirã region

In the Dúrico-Beirã region (Fig. 2a, b), Lower and Medium Cambrian phyllites, alternating with

metagraywackes are overlain, at angular discordance, by Tremadocian-Arenigian metaconglomerates, quartzites, phyllites, metasandstones, graphitic phyllites with intercalations of metavolcanics. Llanvirnian-Llandeilian black slates, phyllites and metagraywackes are unconformably overlain by Ashgillian-Lower Llandoverian graphitic phyllites, metasandstones, metagraywackes and quartzites. These are, in turn, unconformably overlain by Upper Llandoverian graphitic phyllites and metalydites and, unconformably above them, by a sequence of Gedinnian-Siegenian metasandstones, phyllites (Serviços Geológicos de Portugal, 1992; Combes et al., 1992; Couto, 1995).

In the Dúrico-Beirã region (Fig. 2b) Variscan folding gave rise to the large Valongo anticline and a syncline to the west. At Valongo, the anticline has a N31ºW orientation; it rotates to W and, close to Banjas mine, the orientation is N50ºW. In contact with the Castro Daire granites, southwest of Fig. 2b, the orientation is N65ºW. At Valongo-Santa Justa, the axis plunges 10ºNNW. The axial plane dips 60ºNE and the normal anticlinal flank dips 35ºNE. The subvertical inverse flank would have formed during the D_1 Variscan event (Ribeiro et al., 1990). The anticline has second order folds with N32-42ºW orientation and plunges N15ºNW (Combes et al., 1992), probably correlating with the D_2 Variscan event.

In the Dúrico-Beirã region (Fig. 2b), the mines consist of Sb-Au-quartz veins with brecciated structures, up to 200 m long, but their thickness ranges from a few cm to 3.6 m (Table 1). The Sb-ores and gold precipitated in the NE-SW-, NNW-SSE- and ENE-WSW-striking quartz veins which are mainly hosted by the Cambrian phyllites, metagraywackes with intercalations of metaconglomerates and metasandstones (Table 1), although the Variscan faults cut formations of different ages, from Cambrian to Carboniferous (Portugal Ferreira et al., 1971). The Sb-Au-quartz veins outcrop on the limbs of the anticline, filling faults and shear zones normal to the aforementioned structures. Tungsten-tin quartz veins cut the coarse-grained porphyritic biotite-

muscovite granite and appear to be related to it, whereas the Sb-Au quartz veins are distant from granite intrusions. Granite is particularly abundant in the eastern part of the area (Fig. 2b).

3. Samples and analytical methods

Samples were collected from Sb-quartz veins at Moinho do Picão, and Pb-Sb-quartz veins at Cabeço da Mina and Sítio da Coitadinha in the Bragança district, and from Sb-Au quartz veins from Montalto, Pinheirinhos, Abelheira, Medas, Borralhal and Alto do Sobrido in the Dúrico-Beirã region. Our studies included transmitted- and reflected-light microscopy and electron probe microanalysis.

Ore minerals were analyzed on a Cameca Camebax electron microprobe at the Instituto Geológico e Mineiro, S. Mamede de Infesta, Portugal. Analyses were conducted at an accelerating voltage of 15 kV and a beam current of 15 nA. Standards used are Cu (Cu Kα), Ag (Ag Lα), Au (Au Mα), sphalerite (Zn Kα), pyrite (Fe Kα, S Kα), $MnTiO_3$ (Mn Kα), Cd (Cd Lα), Sb (Sb Lα), As (As Lα), galena (Pb Mα) and Bi (Bi Mα). Each element was counted for 20 seconds and ZAF corrections were applied. Backscattered images were obtained using a JEOL JSM 6400, operating at 20 kV, 15 nm and 2.0 nA at the Department of Earth Sciences, University of Manchester, U.K.

Stibnites were chemically prepared for the determination of Pb isotopic data at the State Geological Institute of Dionyztúr in Bratislava, Slovakia. Stibnite samples were digested in nitric acid, evaporated, re-dissolved in hydrobromic acid and put through an AG1 × 8 anion exchange column to purify the Pb. Lead was eluted in 6N HCl. Approximately 1μg of Pb was loaded on an Re filament with silica gel and 1 NH_3PO_4. The Pb isotopic ratios of ten stibnite samples were measured using a static multicollector mode (Faraday collector, 50 ratios, 0.5-1 V signal for ^{208}Pb)

on a VG Sector 54E thermal ionization mass spectrometer (TIMS) at the State Geological Institute of Dionyztúr, Polish Academy of Science, Warsaw, Poland. The mean ratios and total standard deviations observed in eleven analyses of SRM-981 at 1σ are $^{206}Pb/^{204}Pb$=16.941±0.015 (0.09%), $^{207}Pb/^{204}Pb$=15.499±0.020 (0.13%) and $^{208}Pb/^{204}Pb$=36.721±0.063 (0.17%).

4. Mineral associations

Based on our observations and earlier publications (Portugal Ferreira et al., 1971; Santarém Andrade and Portugal Ferreira, 1976; Couto et al., 1990; Noronha et al., 1998), the assemblages for Sb-, Pb-Sb- and Sb-Au deposits in northern Portugal (Figs. 1c, 2b, Table 1) can be classified based on the abundances of the main ore minerals. These assemblages are:

(a) quartz + stibnite for Sb-quartz veins;

(b) quartz + pyrite + galena + berthierite for Pb-Sb-quartz veins; and

(c) three different assemblages for the Sb-Au-quartz veins; I – quartz + sphalerite + stibnite; II – quartz + pyrite + berthierite + stibnite; and III – quartz + arsenopyrite + pyrite + stibnite.

The mineralogy of the studied veins is summarized in Table 2. In each deposit, some minerals show multiple parageneses, suggesting that mineral precipitation was a polyphase process.

The relative abundances of minerals in the Sb-deposit (Moinho do Picão) and Pb-Sb-deposit (Sítio da Coitadinha), in the Bragança district (Fig. 1c), and Sb-Au deposits (Borralhal, Pinheirinhos, Abelheira, Tapada, Ribeiro da Serra, Alto do Sobrido, Ribeiro da Igreja, Vale do Inferno, Medas and Montalto), in the Dúrico-Beirã region (Fig. 2b), are given in Table 2. In the studied deposits, arsenopyrite, pyrite and pyrrhotite are the earliest sulfides to form. Pyrrhotite was, however, not found in the Sb-quartz veins and type I Sb-Au-quartz veins (Table 2). Pyrrhotite is commonly partially transformed into marcasite. The earliest generation of native gold, when found,

is earlier than or contemporaneous with arsenopyrite and earlier than pyrite and pyrrhotite. Sphalerite fills fractures in arsenopyrite, pyrite and pyrrhotite and partly replaces them. At Moinho do Picão, sphalerite contains inclusions of pyrite (Fig. 3a). Chalcopyrite is mainly later than sphalerite, as it partially surrounds sphalerite. At Sítio da Coitadinha, chalcopyrite contains inclusions of pyrite. Galena was found in the Pb-Sb- and Sb-Au-quartz veins and is surrounded by cervantite (Fig. 3b). Rare boulangerite fills fractures in sphalerite. At Ribeiro da Igreja, jamesonite was found to be later than chalcopyrite; electrum is associated with jamesonite (Couto et al., 1990). Rare tetrahedrite fills fractures in sphalerite at Sítio da Coitadinha and Pinheirinhos, and partially surrounds chalcopyrite at Montalto.

A second generation of chalcopyrite was found at Medas, surrounding tetrahedrite. In most of the deposits, a second generation of arsenopyrite was found filling fractures in pyrite I and partially replacing it (Fig. 3c). This later arsenopyrite contains inclusions of pyrite I (Fig. 3d) at Sítio da Coitadinha, and inclusions of tetrahedrite at Pinheirinhos. A second generation of pyrite was found replacing arsenopyrite I. Berthierite is commonly later than both generations of arsenopyrite and pyrite, because it surrounds and partially replaces them, as for example, at Sítio da Coitadinha (Figs. 3c, d). Berthierite also occurs in veinlets with boulangerite where it cuts earlier sulfides. At Montalto, a second generation of boulangerite was found containing inclusions of berthierite and surrounded by plagionite (Fig. 3e). Stibnite is a late sulfide, partially surrounding zoned arsenopyrite (Fig. 3f). In general, stibnite surrounds and penetrates berthierite. However, a later generation of berthierite was found containing inclusions of stibnite. A third generation of pyrite was occasionally found replacing berthierite at Sítio da Coitadinha and Pinheirinhos, and replacing stibnite at Sítio da Coitadinha and Borralhal. Later interstitial stibnite II is observed and is locally accompanied by antimony. Anhedral grains of native gold, ranging from 20 x 20 μm to 70 x 30 μm in size, were found at Pinheirinhos. This gold is present within fractures between arsenopyrite and stibnite, and in stibnite, which is partially replaced by native gold (Figs. 3g, h). Inclusions of gold

rarely occur in quartz (Fig. 3h). Carbonates precipitate in the last hypogene stage. In every deposit, there is also a supergene stage characterized by weathering; cervantite and valentinite were formed (Figs. 3b, i).

5. Comparison of chemical characteristics of ore minerals from Sb- and Sb-Au quartz veins

Sulfides, sulfosalts, native-antimony and gold in samples collected from the selected Sb-, Pb-Sb- and Sb-Au-quartz veins were analyzed to determine their compositions (Table 3). The analyzed arsenopyrites are S-rich and As-poor. As a rule they are microscopically unzoned, except rarely at Pinheirinhos (Fig. 3f), where there is a decrease in S from core to rim. Gold was rarely detected in arsenopyrite and its content is up to 0.12 wt.% at Pinheirinhos and Montalto. The Au content of arsenopyrite does not correlate with As content and this "invisible gold" is therefore considered to occurs as sub-microscopic inclusions of native gold (e.g., Cook and Chryssoulis, 1990). There is a negative correlation between Sb and As in arsenopyrite (Fig. 4a), suggesting that Sb substitutes for As. Furthermore, in the zoned crystals with significant Sb, there is a decrease in Sb and an increase in As from core to rim (Fig. 4b, Table 3), as found in arsenopyrite from Sb- and Pb-Sb quartz veins in the French Massif Central (Bril, 1985) and in some Au-Sb deposits (e.g., Hillgrove, N.S.W., Australia; Ashley et al., 2000).

The Au content of pyrite is up to 0.12 wt.% at Borralhal (Table 3), and does not correlate with any other element. This pyrite does not contain As, which may commonly facilitate incorporation of Au into the pyrite structure (Cook and Chryssoulis, 1990). The elevated Au concentrations (Table 3) are therefore attributed to very small inclusions of gold. The Sb content is only up to 0.04 wt.%. Pyrite has a similar composition in the studied mineralized quartz veins (Figs. 4c, d).

In general, the analyzed berthierites from Sítio da Coitadinha, Abelheira, Medas, Montalto and Borralhal are similar in composition (Fig. 4c, e). Each grain has a homogeneous composition. There are minor substitutions of As for Sb and Mn for Fe in berthierite (Table 3).

In general, sphalerite does not contain Mn or Cu (Table 3), but at Medas and Montalto diffusion-induced segregations of chalcopyrite (Kojima and Sugaki, 1984, 1985; Bente and Doering, 1993) occur. The ranges of mol.% FeS in samples from the same vein are 2 to 3 at Moinho do Picão, 5 to 6 at Sítio da Coitadinha, 0 to 5 at Medas and 3 to 4 at Montalto. Therefore, the compositions of sphalerite from Sb-, Pb-Sb- and Sb-Au-quartz veins are broadly similar. In general, there is no significant variation in the mol.% FeS content within each sphalerite grain, but FeS tends to increase from core to rim in individual sphalerite grains from Moinho do Picão (Table 3). Sphalerite commonly has a low Sb content up to 0.15 wt.%. Chalcopyrite was only found in the Pb-Sb-quartz veins from Sítio da Coitadinha and Sb-Au-quartz veins from Medas and Montalto (Table 3).

Tetrahedrite from Coitadinha and Medas contains up to 2.60 and 3.20 Ag atoms per formula unit (a.p.f.u., calculated on the basis of Au+Cu+Fe+Mn+Zn+Cd=12; Fig. 4f, Table 3), whereas analyzed tetrahedrite from Pinheirinhos and Montalto does not show significant Ag content. The Ag substitutes for Cu (Fig. 4f). The tetrahedrite richest in Ag is also among the richest in Fe and the poorest in Zn. Iron and Zn are commonly present in tetrahedrites in amounts up to 1.91 Fe a.p.f.u. at Medas and 1.78 Zn a.p.f.u. at Montalto, respectively (Fig. 4g). Therefore, there is no chemical distinction in the compositions of tetrahedrite from Pb-Sb-quartz veins and Sb-Au-quartz veins.

Galena has a homogeneous composition (Table 3). Boulangerite $(Pb_{4.83}Cu_{0.02}Ag_{0.01})_{\Sigma 4.86}(Sb_{4.20}As_{0.10})_{\Sigma 4.30}S_{11}$ and plagionite $(Pb_{4.91}Cu_{0.03}Fe_{0.02}Zn_{0.02})_{\Sigma 4.98}(Sb_{8.18}As_{0.15})_{\Sigma 8.33}S_{17}$ were found in Sb-Au-quartz veins from Montalto.

Stibnite has a homogeneous composition (Table 3). It contains up to 1.39 wt.% As in a veinlet cutting other ore minerals at Borralhal. Minor As probably substitutes for Sb (Nakai et al., 1986). Stibnite contains up to 0.14 wt.% Au at Sítio da Coitadinha and Moinho do Picão, and 0.11 wt.% Ag at the latter (Table 3). There is no significant difference in composition between stibnite penetrated by gold and stibnite that is not associated with gold. Furthermore, stibnite from Sb-, Pb-Sb- and Sb-Au-quartz veins has a similar composition. Native antimony is only found at Moinho do Picão and Sítio da Coitadinha (Table 3).

Native gold was only found at Pinheirinhos and contains 95.76 to 99.61 wt.% Au. The grains contain up to 2.62 wt.% Ag, 0.82 wt.% Bi and 0.13 wt.% Sb. Copper, Pb and Fe were also detected (Table 4). Gold grains penetrating between arsenopyrite and stibnite, and also stibnite, are richer in Au and poorer in Ag than those included in quartz (Fig. 4h, i). Furthermore, the former grains have Bi>Ag, while the latter feature Ag>Bi. The fineness [1000 x wt.%Au/(wt.%Au + wt.%Ag); Fischer, 1945] of gold within fractures between arsenopyrite and stibnite and in stibnite ranges between 997 and 1000, which is a higher range than that of gold included in quartz (973 to 977). Gold grains within fractures between arsenopyrite and stibnite and in stibnite from Pinheirinhos have an Ag content similar to that of gold associated with: a) arsenopyrite + pyrite + quartz from Ribeiro da Igreja, b) stibnite + arsenopyrite from Montalto and Tapada, c) berthierite + stibnite from Ribeiro da Serra, and d) late carbonates + stibnite from Tapada (Couto et al., 1990). However, the analyzed gold enclosed in quartz from Pinheirinhos contains less Ag than native gold from Alto do Sobrido and gold and electrum associated with jamesonite + pyrite + sphalerite from Ribeiro da Igreja (Couto et al., 1990).

6. Lead isotope characteristics of stibnite from northern Portugal

Stibnite was selected for the determination of the lead isotope composition because it is the most abundant ore-mineral in all vein types (Table 2). Galena is a major ore-mineral in the Pb-Sb-quartz veins and is locally abundant in type-1 Sb-Au veins; it occurs in trace amounts in types II and III veins (Table 2). The $^{206}Pb/^{204}Pb$ ratio in stibnite from the Bragança district ranges from 18.188 to 18.254 and from 18.158 to 18.520 in specimens from the Dúrico-Beirã region (Table 5). Stibnite from the Dúrico-Beirã region seems to be the most radiogenic (Fig. 5a). The $^{207}Pb/^{204}Pb$ ranges from 15.608 to 15.667 in the Bragança district and from 15.589 to 15.681 in the Dúrico-Beirã region, while $^{208}Pb/^{204}Pb$ ranges from 38.270 to 38.425 and 38.133 to 38.539 in the Bragança district and Dúrico-Beirã region, respectively. In the Pb/Pb diagrams (Fig. 5a, b), the data plot close to the orogenic lead evolution curves of Stacey and Kramers (1975) and Doe and Zartman (1979). The lead μ_2 values of stibnite from Sb and Pb-Sb deposits in the Bragança district range from 9.77 to 10.02, which is similar to the range (9.66 to 10.04) for stibnite from the Sb-Au deposits in the Dúrico-Beirã region (Table 5). These values are consistent with the derivation of the lead from upper crustal sources.

7. Discussion

7.1 Mineralogical and fluid inclusion data

The mineralogy of the Sb- and Pb-Sb-quartz veins from the Bragança district and Sb-Au-quartz veins from the Dúrico-Beirã region shows that stibnite is more abundant than berthierite and that both occur in the last paragenetic stage. The mineralising sequence starts with a Fe-As stage and has intermediate stages consisting of Zn-, Cu- and Pb-sulfides and -sulfosalts. Antimony began to be deposited as traces within arsenopyrite in the first stage, and as tetrahedrite, boulangerite, jamesonite and pyrargyrite, in the intermediate stages, as in the Massif Central and Massif

Armorican in France (e.g., Munoz et al., 1992). Arsenopyrite contains Sb that probably occurs by substitution for As (Fig. 4a). In the zoned crystals, Sb is preferentially accommodated in the core (Fig. 4b), showing that the early As-rich fluids contained some Sb.

A study of fluid inclusions in quartz from the Sb-Au-quartz veins from Ribeiro da Igreja and Ribeiro da Serra in the Dúrico-Beirã region (Couto et al., 1990) showed that the earliest aqueous-carbonic fluids, with CO_2 as the main volatile component, circulated at 290 to 340ºC (fluid inclusion homogenization temperatures). The H_2O-(CO_2) fluids circulated at 230 to 320ºC, whereas the last fluids are aqueous and circulated at ca. 128 to 225ºC. The salinity was low with a constant 2 wt.% equiv. NaCl in the different stages. During the evolution of the quartz veins, there was a significant change from CO_2-bearing metamorphic fluids to dominant aqueous meteoric fluids. The lowest temperatures, decreasing from 225 to 128ºC, correspond to the berthierite- and stibnite-precipitation stage, as also shown by fluid inclusion data in Variscan massive stibnite quartz veins from the French Massif Central and Massif Armorican in France (Munoz et al., 1992) and some Archean Au-As-Sb quartz veins in the Kwekwe district, Zimbabwe (Buchholz et al., 2007). A comparable change in fluid composition was also found in Variscan Au-bearing quartz veins from Laurieras, northern French Massif Central (Essarraj et al., 2001), French Massif Central, NW Iberia and Bohemia (Boiron et al., 2003) and Variscan Au-Sb quartz veins at Monte Ollasteddu, Sardinia (Dini et al., 2005). Studies of fluid chemistry of some Au-bearing veins from the Central Iberian Zone showed that these fluids are very similar to those from barren veins, suggesting that the occurrence of Au-bearing veins are due to factors controlling deposition rather than transport (Murphy and Roberts, 1997).

7.2 Mineralizing environment

Late Variscan fracturing-faulting resulted in formation of Sb±Au deposits in northern Portugal as

in Spain and France (e.g., Mossman et al., 1991; Munoz et al., 1992) and in the Rheinisches Schiefergebirge, NW Germany (e.g., Wagner and Cook, 2000). In the Bragança district, consisting of four main thrust sheets, the Sb- and Pb-Sb-quartz veins mainly intersect Silurian schists belonging to the lower allochthonous sheets (Fig. 1c, Table 1). These veins do not outcrop close to late-orogenic granitic rocks as in German deposits (Wagner and Cook, 2000). Variscan folding, deformation and regional metamorphism occurred in the area (Ribeiro et al., 1990). Collectively, these would have provided the anomalous crustal heat flow required to sustain the extensive and long-lived hydrothermal activity that gave rise to the deep-sourced metamorphic fluids responsible for the mineralized veins.

In the Dúrico-Beirã region, the Sb-Au-quartz veins are the most distant from granite (Fig. 2b). The occurrences of very small amounts of cassiterite, wolframite and scheelite in a few of these veins suggest that they may be genetically linked to the W-Sn deposits, which are closest to granite (Couto et al., 1990). Fractionation of felsic magma may concentrate gold (Neiva and Neiva, 1990; Neiva, 1992).

The CO_2-rich fluids of magmatic-hydrothermal origin in intrusion-related gold deposits associated with W-Sn provinces often have high salinity (e.g., Thompson et al., 1999). However, CO_2-rich fluids with low salinity (2 wt.% NaCl equiv.), like those at the Dúrico-Beirã region, may also signify a magmatic contribution. The early fluids contained some Au, but also Sb, as shown by the arsenopyrite composition (Fig. 4a) and are likely metamorphic in origin. Prograde metamorphism at varying crustal levels would have produced low salinity, CO_2-rich fluids derived from metamorphic devolatilization reactions which flowed upwards along faults and fractures, particularly along shear zones to form ore deposits in cooling (post-metamorphic peak), rocks undergoing uplift. The gold- and stibnite-bearing quartz veins within greenschist facies metamorphic rocks of the Alaskan Cordillera are derived from similar metamorphic fluids

(Goldfarb et al., 1993). The localization of deposits adjacent to shear zones has been considered as evidence for a metamorphic source (e.g., Kyser and Kerrich, 1990; Murphy and Roberts, 1997). Metamorphic fluids from different levels, and also surface fluids, may have mixed. Whether these fluids were suitable for the leaching of ore-forming elements from metasedimentary successions depends on the availability of metal-complexing ligands within the fluid (e.g., Williams-Jones and Normand, 1997; Wood and Samson, 1998). Sulfur was likely abundant within the metasedimentary rocks and was available to hydrothermal fluids at the source of leaching. The deformation responsible for the important shear zones and the associated regional metamorphic event would have provided the anomalous crustal heat flow responsible for the hydrothermal activity that originated the aqueous-carbonic fluids. The latter later mixed with meteoric fluids penetrating the basement from the surface, giving rise to the different paragenetic stages identified in the Sb-Au quartz as the temperature decreased, as at the Castromil gold deposits, northern Portugal (Vallance et al., 2003). However, the only evidence of late meteoric fluids is given by continuously decreasing fluid inclusion homogenization temperatures.

The biotite-muscovite granite from the Dúrico-Beirã region (Fig. 2b) is peraluminous (A/CNK =1.2), late- to post-D_3 and 300±7 Ma in age with a $^{87}Sr/^{86}Sr_0$ ratio of 0.7092±0.0006 (Beetsma, 1995). It is therefore a S-type granite derived by partial melting of a metasedimentary source which probably contained some metals. The late Hercynian granite intrusions would have resulted in a thermal surge that increased the geothermal gradient. Metamorphic-derived fluids and meteoric fluids would have been heated and enriched in metals and could have contributed to the precipitation of ore minerals in quartz veins. As the Sb-Au quartz veins are the most distant from this granite (Fig. 2), the metals derived from the granite magma were retained within the closest veins. In the Alaskan Cordillera, Au- and stibnite-bearing quartz veins occur within metamorphic rocks and were derived from metamorphic fluids; they are close temporally to high-T tectonic deformation and igneous activity (Goldfarb et al., 1993).

Berthierite, stibnite and late native gold belong to the late hypogene stage and could have precipitated from a surface-derived H_2O-NaCl fluid, or more probably from the mixing of the earlier fluids with the late fluids as suggested by Couto et al. (1990) for stibnite, as elsewhere in the European Variscides (Bril, 1982; Boiron et al., 1990).

7.3 Mineral deposition

Arsenopyrite was the earliest sulfide to crystallize. The arsenopyrite with the lowest Sb content was found in the Sb-Au deposits of Pinheirinhos, Borralhal and Montalto in the Dúrico-Beirã region (Fig. 4a). This contained <0.20 wt.% Sb and very low Co and Ni contents. The arsenopyrite composition is independent of fS_2 and is dependent only on temperature in the pyrite stability field (Sharp et al., 1985). Temperatures of 390º and 300ºC are estimated for the first and second generations of arsenopyrite, respectively, in equilibrium with pyrite. They are lower than those estimated for arsenopyrite from Montalto (Couto et al., 1990) and from polymetallic vein (Sb, Pb, Zn, Ag, Cu) of Les Borderies in the French Massif Central (Marcoux et al., 1988). However, some analyzed arsenopyrite grains from the Portuguese Sb-, Pb-Sb- and Sb-Au-deposits studied have Sb ≥ 0.20 wt.% and, consequently, arsenopyrite geothermometry cannot be applied to them (Sundblad et al., 1984).

Sphalerite belongs to a later stage of deposition than stage I arsenopyrite. In general, this sphalerite shows diffusion-induced segregations of chalcopyrite and consequently cannot be used for geobarometry (Bente and Doering, 1993). The difference between the highest and lowest mol.% FeS values of sphalerite in samples from the same vein is < 1 at Sítio da Coitadinha and Moinho do Picão in the Bragança district and up to 1 and 5 at Montalto and Medas, respectively. These evolutionary trends in sphalerite may reflect simultaneous changes in several fluid parameters (T, P,

fO_2, fS_2).

Berthierite formed in the same paragenetic stage as stibnite, but usually before stibnite, as has been noted in deposits of the French Massif Central (Bril, 1982; Bril and Beaufort, 1989) and the Lesser Carpathians, Slovakia (Chovan and András, 1994). The sequence of antimony mineral deposition with decreasing temperature without fO_2 or fS_2 buffering is berthierite followed by stibnite. Berthierite is not found in the Sb-quartz veins and is only a minor phase in type I Sb-Au-quartz veins (Table 2), which is consistent with the absence of a fS_2 buffer. Berthierite is a major phase in the Pb-Sb-quartz veins and type II Sb-Au veins and occurs in large amounts in type III Sb-Au veins (Table 2), because it is fS_2-buffered during cooling. Berthierite continues to precipitate because fS_2 (or fO_2) buffers have equilibrium boundaries approximately parallel to those delineating the stability field of berthierite (Williams-Jones and Normand, 1997).

Stibnite and berthierite are the most important Sb-bearing minerals identified in our study. Stibnite is most abundant, reflecting its greater stability over a wide range of fO_2-pH-T conditions. Berthierite, by comparison, is only stable over extremely narrow intervals of fO_2 and fS_2 (Williams-Jones and Normand, 1997). In general, both ore-minerals are stoichiometric; minor substitutions of As for Sb were found in both, and Mn for Fe in berthierite (Table 3). Stibnite forms relatively late in the paragenetic sequences, as in most stibnite deposits, because at temperatures <250ºC stibnite may precipitate from fluids containing only 1 ppm Sb (Williams-Jones and Normand, 1997). The reaction of ore fluids with slates, a common host for these deposits, enhances reduction of fO_2 which promotes stibnite precipitation (Williams-Jones and Normand, 1997). However, the fluids responsible for stibnite precipitation are typically surface-type H_2O-NaCl fluids, suggesting oxidizing conditions. Therefore, drastic fluid cooling is the most important mechanism for stibnite precipitation. Antimony was carried as an hydroxide complex, because $Sb(OH)_{3(aq)}$ is responsible for hydrothermal transport of Sb, especially at temperatures >200 to 250ºC (Zotov et al., 2003).

Stibnite and berthierite are commonly associated with pyrite because the stability field of stibnite is wholly contained within the field of pyrite; in contrast native antimony is rare, like pyrrhotite (Williams-Jones and Normand, 1997). Both are absent at Borralhal and Pinheirinhos (Table 2). Pyrrhotite and native antimony occur in vein type III, but are not in contact. Native antimony precipitated later than pyrrhotite and there is no textural evidence of equilibrium between pyrrhotite and native antimony in any of the studied deposits. Native antimony is later than stibnite and precipitated at a lower temperature (<200ºC; Williams-Jones and Normand, 1997). Textural observations and data show a stable typology for the system Fe-Sb-S (Williams Jones and Normand, 1997).

The studied Sb-, Pb-Sb- and Sb-Au-quartz veins have a complex paragenesis. They were formed over a relatively wide range of temperatures from about 390 to 128ºC (based on arsenopyrite geothermometry and fluid inclusion data) for the Sb-Au quartz veins. Drastic fluid cooling during the mineralizing event was the most likely cause of mineralization, as in the stibnite and stibnite-gold deposits in the French Massif Central (Bril, 1982; Bril and Beaufort, 1989), Montagne Noire, France (Munoz and Shepherd, 1987), the Moretons Harbour area, Canada (Kay and Strong, 1983), the Lesser Carpathian Mountains (Chovan and András, 1994), the El Juncalón deposits in Spain (Ortega and Vindel, 1995; Ortega et al., 1996) and the Rhenish Massif, Germany (Wagner and Cook, 2000). A decrease in the fluid temperature would significantly reduce Sb solubility, causing stibnite precipitation, as shown experimentally by Krupp (1988). However, deposits showing high stibnite/quartz ratios are likely to have formed through phase separation of originally homogeneous H_2O-CO_2-NaCl fluids like at the Mari Rosa deposit (Ortega and Vindel, 1995).

Different generations of gold were found in the Sb-Au quartz veins from the Dúrico-Beirã region (Couto et al., 1990 and this study). Gold associated with arsenopyrite + pyrite + quartz and electrum

associated with jamesonite are paragenetically earlier and deposited at higher temperature than stibnite, as in the deposits in the Massif Central and some in Bolivia (Dill at al., 1995) and also in Archean deposits (e.g., Hagemann and Lüders, 2003; Buchholz et al., 2007). The metamorphic aqueous carbonic fluid with CO_2 as the main volatile phase, and low salinity (ca. 2 wt.% NaCl equiv.), circulating at 290 to 340ºC (Couto et al., 1990), is responsible for the earliest precipitation of gold. Transport of gold took place as $Au(HS)_2^-$, which is important under neutral pH conditions, while AuHS(aq) is the dominant species in acidic solution (Stefánsson and Seward, 2004). Gold is not transported as monovalent $AuOH_{aq}$, because that is only an important complex at temperatures >400ºC (Stefánsson and Seward, 2004) and is formed in a reduced hydrothermal solution (Stefánsson and Seward, 2003a). Gold is not transported as $Au(Cl)_2^-$, because the chloride complexes play an important role in gold transport in acidic chloride-rich hydrothermal solutions >400ºC (Stefánsson and Seward, 2003b), or in highly oxidized fluids (Gammons and Williams-Jones, 1995).

Electrum belongs to the Pb-Sb paragenetic stage, containing abundant jamesonite, of the Ribeiro da Igreja deposit, where electrum precipitation took place from a H_2O-NaCl (2 wt.% equiv.) - CO_2 fluid, at temperatures of 230 to 320ºC (Couto et al., 1990). Silver is transported as $Ag(HS)_2^-$ under neutral pH conditions, AgHS(aq) in acidic conditions and $Ag_2S(HS)_2^{2-}$ in alkaline solutions (Stefánsson and Seward, 2003c). Therefore, it was likely transported as $Ag(HS)_2^-$ in this case.

A late generation of gold is associated with berthierite and stibnite at Ribeiro da Serra (Couto et al., 1990) and with stibnite at Pinheirinhos (Figs. 4h, i). A H_2O-NaCl (2 wt.% equiv.) surficial-dominant fluid, circulating at 128 to 225ºC (Couto et al., 1990) was responsible for late gold precipitation. Therefore, the mineralized veins display fluid evolution. A relatively alkaline and slightly reducing fluid has potential to be an ore-forming fluid for both Sb and Au deposits

(Williams-Jones and Normand, 1997). Cooling of the near-neutral (or even slightly alkaline) fluid under fluid-buffered conditions will result in a significant decrease of the pH with temperature. Coprecipitation of stibnite and native gold can only occur as a result of the acidification, with or without reduction (Williams-Jones and Normand, 1997). In quartz-stibnite veins, the abundant silicification and precipitation of large amounts of quartz in the initial stages of mineralization might prevent subsequent interaction with the wallrock. The evolved fluid might be confined to fracture zones within the veins themselves, where it could evolve along a fluid-buffered path.

7.4 The source of ore metals

The use of lead isotopes in ore genesis is especially helpful to define the source material of the ore lead. Sulfides and sulfosalts from Sb- and Pb-Sb quartz veins from the Bragança district and Sb-Au quartz veins from the Dúrico-Beirã region have similar isotopic compositions (Fig. 4 and Table 3), suggesting a common origin. Most of the Pb-isotope data (with μ_2 values clustering between 9.76 and 9.89, Table 5) suggest a homogeneous crustal lead source of lead for all three deposit types, which is also supported by the fact that the $^{206}Pb/^{204}Pb$ values for stibnite from the Bragança district are within the range of those for stibnite from the Dúrico-Beirã region (Fig. 5a, b). Two mechanisms are capable of resulting in very homogeneous isotope signatures: (a) magmatic processes, resulting from large scale crustal melting; and (b) hydrothermal processes, through long-lived circulation of fluids in metasedimentary complexes. In the Bragança district, granitic rocks do not crop out close to the studied mineralized veins (Fig. 1c). In the Dúrico-Beirã region, the studied mineralized veins are the most distant from granites (Fig. 2b). Therefore, the host metasediments are the most likely homogeneous source of lead for the ores in both areas. The Pb isotope compositions of stibnite from these deposits can be compared (Fig. 6) with Pb isotope data for Paleozoic detrital sediments of the Central Iberian Zone (Nägler et al., 1993). The data plot close to some of the post-Tremadocian detrital sediments which suffered a Carboniferous anchimetamorphic

overprint which partially homogenized the Pb isotopes of pelites between ~330 and ~320 Ma (Nägler et al., 1993).

Lead isotope compositions of stibnites from Sb-, Pb-Sb- and Sb-Au-quartz veins from the two Portuguese areas are more clustered than those of post-Tremadocian detrital sediments from the Central Iberian Zone (Fig. 6). The sediments are heterogeneous, although they were partially homogenized for Pb isotopes (Nägler et al., 1993). No complementary source is therefore required to explain the isotopic compositions of the Portuguese deposits. The metasediments are several km thick in both Portuguese areas, providing a source for the fluids to leach As, Au, Pb, Sb and other metals, transport them and subsequently form quartz veins. According to Murphy and Roberts (1997), metasediments are the best source of gold mineralization in the Central Iberian Zone. Remobilization of metals from the metasediments would have been related to Variscan metamorphism and deformation, as is the case for polymetallic veins in the French Massif Central (e.g., Marcoux et al., 1988), Sb mineralization in Germany (Wagner and Cook, 2000) and Pb-Sb vein deposits in Cornwall, U.K. (Clayton and Spiro, 2000).

7.5 Comparison with other antimony-gold deposits

In order to compare the relationship of the Pb isotope compositions of stibnite from Sb-, Pb-Sb and Sb-Au quartz veins in northern Portugal with those of comparable deposits, we selected data from the literature on Variscan deposits across Europe, namely Sb-, Pb-Sb- and Au-quartz veins from the French Massif Central and Reinisches Schiefergebirge, Germany (Table 6). The correspondence of the Pb isotope data for these deposits is evident (Fig. 7a, b), supporting that metasediments are the source of Pb (Table 6). Low $^{206}Pb/^{204}Pb$ ratios (Fig. 7a, b) for polymetallic vein ores from Borderies (Marcoux et al., 1988) and three stibnite samples from Germany (Wagner and Schneider, 2002) are attributed to the heterogeneity of Pb isotope compositions, particularly

from different areas. The Portuguese deposits are from two distinct areas and yet show a limited range of Pb isotope compositions, suggesting leaching of Pb from shared basement metasediments. The granite from the Dúrico-Beirã region did not contribute Pb to the system. The Pb isotope compositions of ores are mainly within the framework trends of Stacey and Kramers (1975), as can be seen on Fig. 7a, and are characterized by high $^{208}Pb/^{204}Pb$ relative to $^{207}Pb/^{206}Pb$. The Pb isotope ratios for a stibnite sample from Borralhal plots outside the areas containing most of the data in two diagrams (Fig. 7a, b), while the plot for a stibnite sample from Pinheirinhos only falls outside the main area in Fig. 7a, which is attributed to weathering during the late tectonic movements.

The Pb isotope compositions of the Portuguese ore deposits studied are also compared with those of deposits from Peru, Romania and Sardinia, all containing at least Au or Sb, but having host rocks which are distinct from those of Portuguese deposits (Table 6). All, except those from Sardinia, have higher $^{206}Pb/^{204}Pb$ and $^{208}Pb/^{204}Pb$ ratios than the Portuguese deposits (Fig. 7c, d), suggesting they have distinct origins. The lead source for most of them is interpreted to be mantle and crustal materials (Table 6). In general, $^{207}Pb/^{204}Pb$ values of ores and K-feldspar from the Sardinian Au-Sb quartz veins are higher than those of stibnite from the Portuguese deposits, also indicating a distinct origin. The lead source for the Sardinian deposits consists of metarhyolites and late-Variscan granites. Therefore, Pb from stibnite of Sb-Au-quartz veins from the Dúrico-Beirã region is not derived from the late Variscan granite.

With respect to the origin of the ores, the limited range of Pb isotope compositions from the Bragança district and the Dúrico-Beirã region compared with published data from Sb-, Pb-Sb and Au-deposits from different parts of the world (Table 6 and Fig. 7) indicate the importance of a metasedimentary basement as the source of Pb for the Portuguese deposits.

8. Conclusions

1. In the Portuguese Sb-, Pb-Sb-, and Sb-Au-quartz veins, berthierite and stibnite are the most abundant Sb-bearing minerals; tetrahedrite, boulangerite, plagionite and native antimony also occur.

2. In general, arsenopyrite and pyrite are the earliest sulfides and berthierite and stibnite are late sulfides, which were in turn followed by native antimony. At Pinheirinhos, the analyzed grains of native gold are later than the arsenopyrite and stibnite.

3. Most arsenopyrite contains Sb, which substitutes for As. In single crystals from the Coitadinha, Medas and Pinheirinhos deposits, Sb decreases and As increases from core to rim. First and second generations of arsenopyrite with low Sb contents crystallized at 390 and 300ºC, respectively. The early aqueous-carbonic fluids, with CO_2 as the main volatile, circulated at 340 to 290ºC for the Ribeiro da Igreja Sb-Au deposit (Couto et al., 1990) and are metamorphic fluids.

4. Berthierite is fS_2-buffered during cooling. Stibnite is commonly later than berthierite and precipitated between 225 and 128ºC; native antimony was precipitated at <200ºC. Drastic fluid cooling from 390 to 128ºC is the principal cause of ore precipitation.

5. Ore mineral compositions are similar in the Sb-, Pb-Sb- and Sb-Au-quartz veins indicating that they have a common source.

6. Variscan folding and overthrusts, long deep faults and shear zones in the Bragança district and Dúrico-Beirã region have provided anomalous crustal heat flow to sustain the extensive and long-lived hydrothermal activity that produced the metamorphic fluids derived from the host metasediments. Structural controls are evident for the origin and location of the mineralized veins.

7. Lead isotopic data for stibnite indicate a homogeneous lead source of crustal origin, from a metasedimentary source, for all three types of veins that formed by hydrothermal circulation through the metasedimentary succession. This is consistent with the situation for related deposits of similar type elsewhere in Europe.

Acknowledgments

Thanks are due to Dr. J. Kral for the determinations of Pb isotopic data. A.M.R. Neiva is grateful to Prof. C.M.B. Henderson for the use of the JEOL electron microscope at Manchester University, U.K. Thanks are due to Prof. J.M. Cotelo Neiva for the useful discussions and Prof. N.J. Cook and two anonymous referees for their helpful comments. This research was carried out under a programme of the Geosciences Centre of Coimbra University. P. Andras and A.M.R. Neiva are grateful to the Instituto de Cooperação Científica e Tecnológica Internacional de Portugal for financial support for travel.

References

Ashley, P.M., Creagh, C.J., Ryan, C.C., 2000. Invisible gold in ore and mineral concentrates from the Hillgrove gold-antimony deposits, NSW, Australia. Mineralium Deposita 35, 285-301.

Beetsma, J.J., 1995. The late Proterozoic/Paleozoic and Hercynian crustal evolution of the Iberian Massif, N Portugal. Netherlands Research School of Sedimentary Geology, Publication no. 941108, 223 pp.

Bente, K., Doering, T., 1993. Solid-state diffusion in sphalerites: an experimental verification of the chalcopyrite disease. European Journal of Mineralogy 5, 465-478.

Boiron, M.-C., Cathelineau, M., Banks, D.A., Fourcade, S., Vallance, J., 2003. Mixing of metamorphic and surficial fluids during the uplift of the Hercynian upper crust: consequences for gold deposition. Chemical Geology 194, 119-141.

Boiron, M.C., Cathelineau, M., Debussy, J., Bastoul, A.M., 1990. Fluids in Hercynian Au veins from the French Variscan belt. Mineralogical Magazine 54, 231-243.

Bril, H., 1982. Fluid inclusions study of Sn-W-Au, Sb- and Pb-Zn mineralizations from the Brionde-Massiac district (French Massif Central). Tschermaks Mineralogische und Petrographische Mitteilungen 30, 1-16.

Bril, H., 1985. Conditions of stabilité des sulfures dans les filons de haute température du district Brioude-Massiac (Massif Central français). Bulletin de Minéralogie 108, 161-171.

Bril, H., Beaufort, D., 1989. Hydrothermal alteration and fluid circulation related to W, Au, Sb vein mineralizations, Haut Alher, Massif Central, France. Economic Geology 84, 2237-2251.

Buchholz, P., Oberthür, T., Lüders, V., Wilkinson, J., 2007. Multi stage Au-As-Sb mineralization and crustal-scale fluid evolution in the Kwekwe district, Midlands greenstone belt, Zimbabwe: a combined

geochemical, mineralogical, stable isotope, and fluid inclusion study. Economic Geology 102, 347-378.

Carvalho, A.D. de, 1981. Recuperação de antigas explorações mineiras. Congresso 81 da Ordem dos Engenheiros, Lisboa, p. 1-9.

Chovan, M., András, P., 1994. Sb, Au-mineralization in the Malé Karpaty Mts. In: Chovan, M., Háber, A., Jeleň, S., Rojkovič, I, (Eds.), Ore textures in the western Carpathian: Bratislava, Slovak Academic Press, p. 60-68.

Clayton, R.E., Spiro, B., 2000. Sulphur, carbon and oxygen isotope studies of early Variscan mineralization and Pb-Sb vein deposits in the Cornubian orefield: implications for the scale of fluid movements during Variscan deformation. Mineralium Deposita 35, 315-331.

Combes, A., Cassard, D., Couto, H., Damião, J., Ferraz, P., Urien, P., 1992. Caractérisation structurale des minéralisations auriféres d'Arénigien dans la région de Valongo (Baixo Douro, Portugal). Chronique de la Recherche Minière 509, 3-15.

Cook, N.J., Chryssoulis, S.L., 1990. Concentrations of "invisible gold" in the common sulfides. Canadian Mineralogist 28, 1-16.

Couto, H., 1995. As mineralizações de Sb-Au da região Dúrico-Beirã: controlos das mineralizações, hipóteses genéticas e relação com mineralizações de Pb-Zn (Ag) e Sn-W. Memórias do Museu e Laboratório Mineralógico e Geológico, Faculdade de Ciências, Universidade do Porto 4, 541-546.

Couto, H., Roger, G., Moëlo, Y., Brill, H., 1990. Le district à antimoine-or Dúrico-Beirão (Portugal): évolution paragénétique et géochimique; implications méttalogéniques. Mineralium Deposita 25 (Suppl.), 569-581.

Dill, H.G., 1998. Evolution of Sb mineralisation in modern fold belts: a comparison of the Sb mineralisation in the central Andes (Bolivia) and the Western Carpathians (Slovakia). Mineralium Deposita 33, 359-378.

Dill, H.G., Weiser, T., Bernhardt, I.R., Kilibarda, C.R., 1995. The composite gold-antimony vein deposit at Kharma (Bolivia). Economic Geology 90, 51-66.

Doe, B.R., Zartman, R.E., 1979. Plumbotectonics I, the Phanerozoic. In: Barnes, H.E. (Ed.), Geochemistry of hydrothermal ore deposits, John Wiley and Sons, New York, p. 22-70.

Dini, A., Vincenzo, G.D., Ruggieri, G., Rayner, J., Lattanzi, P., 2005. Monte Ollasteddu, a new discovery in the Variscan basement of Sardinia (Italy): first isotopic (^{40}Ar-^{39}Ar, Pb) and fluid inclusion data. Mineralium Deposita 40, 337-346.

Essaraj, S., Boiron, M.-C., Cathelineau, M., Fourcade, S., 2001. Multistage deformation of Au-quartz veins (Laurieras, French Massif Central): evidence for late gold introduction from microstructural, isotopic and fluid inclusion studies. Tectonophysics 336, 79-99.

Fischer, N.H., 1945. The fineness of gold with special reference to the Morobe goldfield, New Guinea. Economic Geology 40, 449-495.

Gammons, C.H., Williams-Jones, A.E., 1995. The solubility of Au-Ag alloy + AgCl in HCl/NaCl solutions at 300ºC: New data on the stability of Au(I) chloride complexes in hydrothermal fluids. Geochimica et Cosmochimica Acta 59, 3453-3468.

Gibbons, W., Moreno, T., 2002. Introduction and overview. In: Gibbons, W., Moreno, T. (Eds.), The Geology of Spain. Geological Society of London, p. 1-6.

Gökce, A., Spiro, B., 1994. Stable isotope study of antimony deposits in the Muratdagi region, western Turkey. Mineralium Deposita 29, 361-365.

Goldfarb, R.J., Snee, L.W., Pickthorn, W.J., 1993. Orogenesis, high-T thermal events, and gold vein formation within metamorphic rocks of the Alaskan Cordillera. Mineralogical Magazine 57, 375-394.

Gumiel, P., 1983. Metalogenia de los yacimientos de Sb de la Peninsula Ibérica. Tecniterrae 27, 6-120.

Gumiel, P., Arribas, A., 1987. Antimony deposits in the Iberian Peninsula. Economic Geology 82, 1453-1463.

Hagemann, S.G., Lüders, V., 2003. P-T-X conditions of hydrothermal fluids and precipitation mechanism of stibnite-gold mineralization at the Wiluna lode-gold deposits, Western Australia: conventional and infrared microthermometric constraints. Mineralium Deposita 38, 936-952.

Huston, D.L., Blewett, R.S., Keillor, B., Standing, J., Smithies, R.H., Marshall, A., Mernagh, T.P., Kamprad, J., 2002. Lode gold and epithermal deposits of the Mallina Basin, North Pilbara Terrain, Western Australia. Economic Geology 97, 801-818.

Hutchison, C.S., 1983. Economic deposits and their tectonic setting. Macmillan, Hong Kong, 365 pp.

Kay, A., Strong, D.F., 1983. Geologic and fluid controls on As-Sb-Au mineralization in the Moretons Harbour area, Newfoundland. Economic Geology 78, 1590-1604.

Kojima, S., Sugaki, A., 1984. Phase relations in the central portion of the Cu-Fe-Zn-S system between 800ºC and 500ºC. Mineralogical Journal 12, 15-28.

Kojima, S., Sugaki, A., 1985. Phase relations in the Cu-Fe-Zn-S system between 500ºC and 300ºC under

hydrothermal conditions. Economic Geology 80, 158-171.

Kontak, D.J., Cumming, G.L., Krstic, D., Clark, A.H., Farrar, E., 1990. Isotopic composition of lead in ore deposits of the Cordillera Oriental, southeastern Peru. Economic Geology 85, 1584-1603.

Kontak, D.J., Horne, R.J., Smith, P.K., 1996. Hydrothermal characterization of the West Gore Sb-Au deposit, Meguma Terrane, Nova Scotia, Canada. Economic Geology 91, 1239-1262.

Krupp, R.E., 1988. Solubility of stibnite in hydrogen sulfide solutions, speciation, and equilibrium constants, from 25 to 350º C. Geochimica et Cosmochimica Acta 52, 3005-3015.

Kyser, T.K., Kerrich, R., 1990. Geochemistry of fluids in tectonically active crustal regions. In: Nesbitt, B.E. (Ed.), Short course on fluids in tectonically active regimes of the continental crust. Mineralogical Association of Canada Short Course Handbook 18, 133-230.

Marcoux, E., Bril, H., 1986. Heritage et sources des metaux d'apres la geochimie isotopique du plomb. Mineralium Deposita 21, 35-43.

Marcoux, E., Grancea, L., Lupulescu, M., Milési, J.P., 2002. Lead isotope signatures of epithermal porphyry-type ore deposits from the Romanian Carpathian Mountains. Mineralium Deposita 37, 173-184.

Marcoux, E., Moelo, Y., Picot, P., Baubron, J-C, 1988. Evolution mineralogique et isotopique (Pb) du filon sulfuré complexe des Borderies (Massif Central français) – implications métalogéniques. Mineralium Deposita 23, 58-70.

Marcoux, E., Picot, P., Moëlo, Y., 1985. Evolution paragénétique des minéralisations sulfurées aurifères du district de Pontvieux-Labessette (Puy-de-Dôme). Apport des études isotopiques du plomb. Bulletin de Minéralogie 108, 465-481.

Mossman, D.J., Leblanc, M.L., Burzynski, J.F., 1991. Antimony-gold deposits of North Atlantic Acadian-Hercynian domain. Transactions of the Institution of Mining and Metallurgy 100, B227-B233.

Munoz, M., Shepherd, T.Y., 1987. Fluid inclusion study of the Bournac polymetallic (Sb-As-Pb-Zn-Fe-Cu …) vein deposit (Montagne Noire, France). Mineralium Deposita 22, 11-17.

Munoz, M., Courjault-Radé, P., Tollon, F., 1992. The massive stibnite veins of the French Palaeozoic basement: a metallogenic marker of Late Variscan brittle extension. Terra Nova 4, 171-177.

Mukasa, S., Vidal, C.E., Injoque-Espinoza, J., 1990. Pb isotope bearing on the metallogenesis of sulfide ore deposits in central and southern Peru. Economic Geology 85, 1438-1446.

Murphy, P.J., Roberts, S., 1997. Evolution of a metamorphic fluid and its role in lode gold mineralisation in

the Central Iberian Zone. Mineralium Deposita 32, 459-474.

Nägler, T.F., Schäfer, H-J., Gebauer, D., 1993. A new approach for the determination of the age of partial or complete homogenization of Pb isotopes – Example: anchimetamorphic, detrital sediments of the Central Iberian Zone, Spain. Chemical Geology (Isotope Geoscience Section) 107, 191-199.

Nakai, I., Yokoi, H., Nagashima, K., 1986. Crystal chemistry of the system As-Sb-S(I): Synthesis of wakabeyashilite and synthetic study on the solid solutions in the As_2S_3-Sb_2S_3 system. Mineralogical Journal 13, 212-222.

Neiva, A.M.R., 1992. Geochemistry and evolution of Jales granitic system, northern Portugal. Chemie der Erde 52, 225-241.

Neiva, J.M.C., 1956. Considerations sur la geochemie de blendes et de galenes portugaises. Estudos, Notas e Trabalhos do Serviço de Fomento Mineiro 11, 204-235.

Neiva, J.M.C., Neiva, A.M.R., 1990. The gold area of Jales (northern Portugal). Terra Nova 2, 243-254.

Noronha, F., Ramos, J.M.F., Moreira, A., Oliveira, A.F.M., 1998. Mineralizações filonianas de chumbo-antimónio do NE de Portugal. Algumas notas para o seu conhecimento. Actas do V Congresso Nacional de Geologia, Comunicações do Instituto Geológico e Mineiro 84, B75-B78.

Ortega, L., Oyarzun, R., Gallego, M., 1996. The Mari Rosa late Hercynian Sb-Au deposit, western Spain. Mineralium Deposita 31, 172-187.

Ortega, L., Vindel, E., 1995. Evolution of ore-forming fluids associated with late Hercynian antimony deposits in central/western Spain: Case study of Mari Rosa and El Juncalón. European Journal of Mineralogy 7, 655-673.

O'Shea, P.J., Pertzel, B.A., 1988. The Brunswick gold-antimony mine, Costerfield, Victoria. Geological Society of Australia Abstract Series 23, 282-284.

Pitcairn, I.K., Teagle, D.A.H., Craw, D., Olivo, G.R., Kerrich, R., Brewer, T.S., 2006. Sources of metals and in orogenic gold deposits: insights from the Otago and Alpine schists, New Zealand. Economic Geology 101, 1525-1546.

Portugal Ferreira, M., Santos Oliveira, J.M., Santarém Andrade, R., 1971. Ocorrências de antimónio no Norte de Portugal. Congresso Hispano-Luso-Americano Geologia Económica 1º, Madrid-Lisboa t1, 597-617.

Ribeiro, A., 1974. Contribution à l'étude-téctonique de Trás-os-Montes oriental. Memórias dos Serviços

Geológicos de Portugal (Nova Série) 24, 168 pp.

Ribeiro, A., Pereira, E., Dias, R., 1990. Allochthonous sequences: structure in the northwest of the Iberian Península. In: Dalmeyer, R.D., Garcia, E.M. (Eds.), Pre-Mesozoic Geology of Iberia, Springer-Verlag, Berlin-Heidelberg, p. 220-236.

Santarém Andrade, R., Portugal Ferreira, M., 1976. Distrito antimonífero Dúrico-Beirão: mineralização de SB-Zn-Pb no jazigo de Ribeiro da Igreja (Valongo, Norte de Portugal). Memórias, Notícias e Publicações do Museu e Laboratório Mineralógico e Geológico da Universidade de Coimbra 82, 67-77.

Serviços Geológicos de Portugal, 1992. Portuguese geological map 1/500 000.

Sharp, Z., Essene, E.J., Kelly, W.C., 1985. A re-examination of the arsenopyrite geothermometer: pressure considerations and applications to natural assemblages. Canadian Mineralogist 23, 517-534.

Stacey, J.S., Kramers, J.D., 1975. Approximation of terrestrial lead isotope evolution by a two stage model. Earth and Planetary Science Letters 26, 207-221.

Stefánsson, A., Seward, T.M., 2003a. The hydrolysis of gold (I) in aqueous solutions to 600º C and 1500 bar. Geochimica et Cosmochimica Acta 67, 1677-1688.

Stefánsson, A., Seward, T.M., 2003b. Stability of chloridogold (I) complexes in aqueous solutions from 300 to 600º C and from 500 to 18000 bar. Geochimica et Cosmochimica Acta 67, 4559-4576.

Stefánsson, A., Seward, T.M., 2003c. Experimental determination of the stability and stoichiometry of sulphide complexes of silver (I) in hydrothermal solutions to 400º C. Geochimica et Cosmochimica Acta 67, 1395-1413.

Stefánsson, A., Seward, T.M., 2004. Gold (I) complexing in aqueous sulphide solutions to 500ºC at 500 bar. Geochimica et Cosmochimica Acta 68, 4121-4143.

Sundblad, K., Zachrisson, E., Smeds, S-A., Berglund, S., Alinder, C., 1984 Sphalerite geobarometry and arsenopyrite geothermometry applied to metamorphosed sulfide ores in the Swedish Caledonides. Economic Geology 79, 1660-1668.

Thompson, J.F.H., Sillitoe, R.H., Baker, T., Lang, J.R., Mortensen, J.K., 1999. Intrusion-related gold deposits associated with tungsten-tin provinces. Mineralium Deposita 34, 323-334.

Vallance, J., Cathelineau, M., Boiron, M.C., Fourcade, S., Shepherd, T.Y., Naden, J., 2003. Fluid-rock interactions and the role of late Hercynian aplite intrusion in the genesis of the Castromil gold deposit, northern Portugal. Chemical Geology 194, 201-224.

Wagner, T., Cook, N.J., 2000. Late-Variscan antimony mineralization in the Rheinisches Schiefergebirge, NW: evidence for stibnite precipitation by drastic cooling of high-temperature fluid systems. Mineralium Deposita 35, 206-222.

Wagner, T., Schneider, J., 2002. Lead isotope systematics of vein-type antimony mineralization, Reinisches Schiefergebirge, Germany: a case history of complex reaction and remobilisation processes. Mineralium Deposita 37, 185-197.

Williams-Jones, A.E., Normand, C., 1997. Controls of mineral parageneses in the system Fe-Sb-S-O. Economic Geology 92, 308-324.

Wood, S.A., Samson, I.M., 1998. Solubility of ore minerals and complexation of ore metals in hydrothermal solutions. Reviews in Economic Geology 10, 33-80.

Zotov, A.V., Shikina, N.D., Akinfiev, N.N., 2003. Thermodynamic properties of the Sb (III) hydroxide complex $Sb(OH)_{3(aq)}$ hydrothermal conditions. Geochimica et Cosmochimica Acta 67, 1821-1836.

Figure captions

Fig. 1. (a) The Galiza and Trás-os-Montes Zone and Central Iberian Zone of the Iberian Massif and locations of the Bragança district and Dúrico-Beirã region. (b) Location of Fig. 1c on the map of Portugal. (c) Simplified geological map of NE Portugal (adapted from the geological map of Portugal; Serviços Geológicos de Portugal, 1992).

Fig. 2. (a) Location of Fig. 2b on the map of Portugal. (b) Geological map of the Dúrico-Beirã region (adapted from Couto et al., 1990).

Fig. 3. Back-scattered electron images of ore minerals, some of their alteration products, and muscovite of Sb-, Pb-Sb- and Sb-Au quartz veins from northern Portugal. (a) Pyrite (Py) included in sphalerite (Sph); sphalerite surrounding quartz (Q) and apatite (Ap); scorodite (Sco) surrounding stibnite (St) and sphalerite from Moinho do Picão. (b) Arsenopyrite (Ars), galena (Gl) and antimony (Sb) surrounded by cervantite (Cer); stibnite surrounding galena from Coitadinha. (c) Arsenopyrite (partially replaces pyrite); berthierite (Bt) surrounding arsenopyrite, pyrite and stibnite; stibnite partially surrounds arsenopyrite from Coitadinha. (d) Arsenopyrite with inclusions of pyrite; berthierite replacing arsenopyrite and pyrite from Coitadinha. (e) Boulangerite (Bl) with inclusions of berthierite and partially surrounded by

plagionite (Pl) occur in a miarolitic cavity among euhedral quartz crystals from Montalto. (f) Slightly zoned arsenopyrite with inclusions of quartz and partially surrounded by stibnite from Pinheirinhos. (g) Gold (Au) penetrating between arsenopyrite and stibnite and along fractures in stibnite and partially replacing stibnite; stibnite surrounding arsenopyrite and pyrite from Pinheirinhos. (h) Gold surrounding rutile (Rt) and partially arsenopyrite; gold penetrating along fractures and partially replacing stibnite and quartz; rare gold included in quartz; stibnite surrounding euhedral crystals of quartz from Pinheirinhos. (i) Valentinite (Vi) penetrating muscovite.

Fig. 4. Compositions of some ore-minerals in Sb-, Pb-Sb- and Sb-Au-quartz veins from northern Portugal. (a) and (b) Correlation between Sb and As in arsenopyrite; (b) showing the distribution of Sb and As from core to rim of single zoned crystals of arsenopyrite; As increases and Sb decreases from core to rim. (c) S-Fe-(As+Sb) diagram showing the positions of diagrams (d) and (e); (d) pyrite, (e) berthierite. (f) and (g) Inter-element correlations (atoms per formula unit) in tetrahedrite; (f) between Ag and Cu; (g) between Zn and Fe. (h) and (i) Compositions of gold grains from Pinheirinhos plotted on the Au-Ag-Bi diagram; (h) shows the location of (i); the gold grains included in quartz are the poorest in Au and the richest in Ag. The ore mineral compositions are similar in Sb-, Pb-Sb- and Sb-Au-quartz veins.

Fig. 5. $^{207}Pb/^{204}Pb$ *vs.* $^{206}Pb/^{204}Pb$ plots of stibnite Pb-isotopes from deposits in northern Portugal. Framework trends are plotted for reference (Stacey and Kramers, 1975). These isotopic data suggest a homogeneous crustal source of lead for these deposits.

Fig. 6. Pb isotopic compositions of stibnite from deposits in northern Portugal and of Paleozoic sediments of the Central Iberian Zone, Spain (Nägler et al., 1993). The stibnite data plot close to some of the post-Tremadocian detrital sediments.

Fig. 7. $^{207}Pb/^{204}Pb$ *vs.* $^{206}Pb/^{204}Pb$ and $^{208}Pb/^{204}Pb$ *vs.* $^{206}Pb/^{204}Pb$ diagrams for ores from Sb, Pb-Sb, Sb-Au and polymetallic deposits from various regions of the world to compare with those of stibnite from Bragança district and Dúrico-Beirã region. (a) and (b), French Massif Central: Sb, Pb-Sb quartz veins (Marcoux and Bril, 1986); polymetallic veins (Marcoux et al., 1988); Au-bearing quartz veins (Marcoux et al., 1985) and Sb-quartz veins and (Cu)-Pb-Sb sulfosalt assemblages, Rheinisches Massif, Germany (Wagner and Schneider, 2002). Framework trends are plotted for reference (Stacey and Kramers, 1975). (c) and (d). Peru: polymetallic veins, Au-bearing quartz veins (Mukasa et al., 1990); Sb-W veins (Kontak et al., 1990); Au-polymetallic veins (Marcoux et al., 2002; Au-Sb quartz veins (Dini et al., 2005). The

metasedimentary basement is the source of Pb for the studied Portuguese deposits, consistent with the situation for related ores elsewhere in Europe.

Table 1
Characteristics of the most important antimony, lead-antimony and antimony-gold quartz veins from the Bragança district and Dúrico-Beirã region, northern Portugal

Bragança district				
Antimony quartz veins	Orientations of veins	Thickness	Au and Ag grades	Country rock
Vale da Mulher, Canedo, Pombeiro (Outeiro, Bragança)	N65º-90ºW, 70ºSSW-90º-68ºNNE	0.10-0.60 m	2.2 g/t Ag, 9.5 g/t Ag at Canedo and Pombeiro, respectively	Parautochthonous thrust complex (Silurian to possible Lower Devonian graphitic phyllites, metatuff, metagraywackes and quartzites)
Cabecinha do Prado (Vilar do Chão, Alfândega da Fé)	N65º-90ºW, 70ºSSW-90º-68ºNNE	0.20 m frequent	1.7 g/t Au, 4.0 g/t Ag at Fonte Limpa	
Moinho da Gralheira, Gralheira, Ribeiro de Maçãs (Algoso, Vimioso)	N65º-90ºW, 70ºSSW-90º-68ºNNE N0º-22ºW,70º-85ºENE	0.10	Traces of Au	Lower allochthonous thrust complex (Ordovician-Silurian-Lower Devonian augengneisses, quartzites, phylittes, hematitic phyllites with intercalations of marble and acid and basic metavolcanics)
Serrinha (Mogadouro)	N40-60E, 65º-75ºNW	0.10-0.30 m		
Picão (Moinho do Picão)	N40º-70ºE, 80ºNW-90º-60ºSE	0.15-1.30 m		
Vale do Ninho (Mascarenhas, Mirandela)	N45ºW, 20ºNE	< 0.5 m		
Lead-antimony quartz veins	Orientations of veins	Thickness	Au and Ag grades	Country rock
Sítio da Coitadinha (Grijó de Valebemfeito, Macedo de Cavaleiros)	N80ºE, 80ºN	0.30 m	2-22 g/t Au and 28-280 g/t Ag	Lower allochthonous thrust complex (Ordovician-Silurian-Lower Devonian augengneisses, quartzites, phyllites, hematitic phyllites with intercalations of marble and acid and basic metavolcanics)
Cabeço da Mina (Campo de Víboras, Vimioso)	N50ºW, 80ºSW	0.10-0.60 m		

Table 1 continued

Dúrico-Beirã region				
Antimony-gold quartz veins	Orientations of veins	Thickness	Au and Ag grades	Country rock
Ribeiro da Igreja	N32º-50ºE, 50ºSE N69º-76ºE, 50ºSE N70º-90ºE, 50ºSSE (the main vein)	≤ 0.30 m > 1 m > 1 m	5 g/t Au, but locally 20-40 g/t Au	Early and Middle Ordovician metaconglomerates, quartzites, metasandstones, graphitic phyllites with metavolcanic intercalations
Vale do Inferno	N65º-80ºW, 75ºNNE N0º-24ºE, 70ºE	up to 1 m 0.10 – 1 m	up to 5 g/t Au	Cambrian phyllites and metagraywackes with intercalations of metaconglomerates and metasandstones
Abelheira	N30ºE, 60ºWNW	0.8 m		
Medas	N30ºE, 60ºWNW	0.3-1.20 m		Cambrian phyllites and metagraywackes with intercalations of metaconglomerates and metasandstones
Montalto	N30º-45ºW, > 50ºSW N80º-90ºW	0.40-0.50 m up to 1.5 m	60-180 g/t; reaching 500 g/t Au 20-460 g/t Ag	
Borralhal	N20ºE, 60ºWNW	0.2 m		Cambrian phyllites and metagraywackes with intercalations of metaconglomerates and metasandstones
Pinheirinhos	N40º-50ºE, 70ºSE	up to 3.6 m	up to 6 g/t Au	
Tapada	N80º90ºE, 25ºS N52ºE	0.80 m	6-45 g/t Au	Cambrian phyllites and metagraywackes with intercalations of metaconglomerates and metasandstones
Ribeiro da Serra	N-S N10ºE, 20º-60ºW (main vein) N70ºE, 70º-80ºNNW E-W, 70º-80ºN E-W, 40º-65ºN	0.10-0.15 m 0.70 m	2-45 g/t Au	Cambrian phyllites and metagraywackes with intercalations of metaconglomerates and metasandstones
Alto do Sobrido	N80ºE-70ºN N37º-80ºE, 54-80ºNW N35º-52ºE, 80ºSE-90º-80ºNW N53º-70ºE, 70ºSE-90º-70ºNW N83º-100ºE, 52ºN-90º-48ºS N73º-75ºE, 78º-80ºSSW N73º-75ºS, 75º-78ºSSE	 up to 1.5 m up to 1.5 m	 up to 7 g/t Au	Cambrian phyllites and metagraywackes with intercalations of metaconglomerates and metasandstones; Stephanian Carboniferous breccia conglomerate

Table 2
Mineralogical characteristics of the antimony and antimony-gold quartz veins from northern Portugal

Mineral	Vein type				
	Sb	Pb-Sb	Sb-Au		
			I	II	III
quartz	M	M	M	M	M
sphalerite	m	m	M	t	L to m
stibnite	M	L	M	M	M
berthierite	—	M	m	M to L	L
arsenopyrite	t	L	L	L to m	M to L
galena	—	M to L	L	t	t
pyrite	t	M	L	M	M to L
marcasite	—	—	m	t	t
chalcopyrite	—	m	m	t	m to t
tetrahedrite	—	m	m	t	t
carbonates	—	—	m	t	m
rutile	—	t	t	t	t
cassiterite	—	—	t	—	t
gold	—	—	t	t	m to t
pyrrhotite	—	t	—	t	m
boulangerite	—	—	t	t	t
bournonite	—	—	—	F	t
antimony	t	t	—	t	m
jamesonite	—	—	—	t	L to m
stannite	—	—	—	—	m
copper	—	—	—	—	m
plagionite	—	—	—	m	t
wolframite	—	—	—	—	t
pyrargyrite	—	—	—	—	t
zinkenite	—	—	—	t	t

Sb veins – Moinho do Picão, Pb-Sb veins – Coitadinha from Bragança district (Fig. 1c); Sb-Au veins: I – Borralhal and Pinheirinhos, II – Abelheira, Tapada, Ribeiro da Serra and Alto do Sobrido, III – Ribeiro da Igreja, Vale do Inferno, Medas and Montalto of the Dúrico-Beirã region (Fig. 2b).

M – major, L – locally abundant, m – minor, t – traces, — not found. In II, m for arsenopyrite at Ribeiro da Serra and Alto do Sobrido and for berthierite at Alto do Sobrido. In III, m for sphalerite and jamesonite and t for chalcopyrite at Vale do Inferno; L for arsenopyrite and pyrite , t for chalcopyrite and m for jamesonite at Montalto. Traces for cassiterite were found at Pinheirinhos (I), traces of cassiterite and wolframite at Ribeiro da Igreja (III) (Couto et al., 1990) and wolframite at Vale do Inferno (III) (Neiva, 1944).

Table 3
Selected electron-microprobe chemical analyses in wt.% of some sulfides, sulfosalts and antimony of antimony, lead-antimony and antimony-gold quartz veins from northern Portugal

		Cu	Ag	Au	Zn	Fe	Mn	Cd	Sb	As	Pb	Bi	S	Total
Arsenopyrite														
core	Coitadinha	—	—	—	0.08	34.97	—	0.04	0.77	41.88	—	—	22.55	100.30
rim		—	—	—	0.04	33.91	—	0.26	0.11	43.50	—	—	21.74	99.57
	Pinheirinhos	0.04	—	—	—	36.08	—	—	0.68	40.67	—	—	22.69	100.16
core		0.10	0.09	—	—	34.64	0.04	0.03	1.13	40.70	—	—	23.33	100.06
rim		—	0.04	—	—	35.59	0.04	—	0.12	43.20	—	—	21.08	100.07
	Medas	—	0.07	—	0.16	34.74	0.04	0.07	3.28	39.53	—	—	22.61	100.50
Pyrite	Borralhal	0.11	—	0.12	—	46.77	—	—	—	—	—	—	53.08	100.09
Berthierite	Borralhal	0.04	—	—	0.16	12.99	0.08	—	56.82	0.81	—	—	29.08	99.98
Sphalerite	Medas	—	0.06	—	62.33	2.96	0.06	0.17	0.29	0.05	—	0.13	33.43	99.48
	Coitadinha	—	0.03	—	62.39	3.17	—	—	0.05	—	—	—	34.06	99.70
	Montalto	—	—	—	66.31	—	—	0.97	—	—	—	—	32.44	99.74
core	Moinho do Picão	—	—	—	68.35	1.31	0.08	0.03	—	—	—	—	30.81	100.54
rim	Moinho do Picão	—	—	—	66.48	1.93	—	0.11	—	—	—	—	31.12	99.73
Chalcopyrite	Coitadinha	34.18	—	—	0.48	30.65	—	—	0.36	0.04	—	—	34.04	99.77
	Medas	33.07	—	—	—	30.86	0.04	—	0.44	—	—	—	35.04	99.80
	Montalto	34.19	—	—	0.19	29.83	0.03	—	0.04	0.05	—	—	35.81	100.14
Tetrahedrite	Coitadinha	25.64	15.52	—	2.72	4.19	—	—	27.99	0.45	—	—	22.83	99.34
	Medas	23.07	18.92	—	1.01	5.48	—	—	27.33	0.43	—	—	23.23	99.48
	Pinheirinhos	37.69	—	—	2.53	4.95	0.04	—	28.99	0.54	—	—	25.23	100.00
	Montalto	35.80	0.32	—	6.72	1.37	—	—	30.23	0.49	—	—	24.77	99.72
Galena	Coitadinha	0.10	—	—	0.14	0.08	0.04	0.04	0.03	—	85.22	—	14.25	99.93
Boulangerite	Montalto	0.05	0.07	—	—	—	—	—	27.34	0.41	53.55	—	18.85	100.29
Plagionite	Montalto	0.07	—	—	0.05	0.05	—	—	38.71	0.44	39.55	—	21.17	100.04
Stibnite	Borralhal	0.05	—	0.04	0.11	0.13	—	—	71.06	1.39	—	—	27.13	99.91
	Alto do Sobrido	0.03	—	0.03	—	0.04	0.08	—	69.68	1.04	—	—	29.00	99.82
	Coitadinha	0.08	—	0.14	—	0.05	0.07	—	69.53	0.87	—	0.03	28.83	99.61
	Moinho do Picão	0.06	0.11	0.14	0.03	—	—	0.04	71.63	0.99	—	0.13	27.07	100.20
Antimony	Moinho do Picão	0.07	0.04	—	0.03	0.04	0.03	—	97.87	1.81	0.06	—	—	100.02
	Coitadinha	0.06	—	—	—	0.50	0.11	—	97.47	1.94	—	—	0.12	100.20

The minimum detection limit for all elements is 200 ppm. — Less than the minimum detection limit.

Table 4
Electron microprobe analyses in wt.% of gold grains from Pinheirinhos

	Penetrating between arsenopyrite and stibnite	Penetrating stibnite	Included in quartz
N. of grains	6	4	4
Au	99.05	98.85	96.24
Ag	0.11	0.22	2.51
Bi	0.70	0.61	0.61
Sb	—	—	0.03
Fe	0.10	0.07	—
Cu	0.02	0.04	0.13
Pb	—	0.06	0.02
Total	99.98	99.85	99.54
Ranges of :			
Au, wt.%	99.85 – 99.61	98.47 – 99.18	95.76 – 96.82
Ag, wt.%	0 – 0.16	0.15 – 0.30	2.32 – 2.62
Bi, wt.%	0.65 – 0.82	0.50 – 0.76	0.48 – 0.73
Fineness	997 – 1000	997 – 998	973 – 977

N – number; — not detected.

Table 5
Stibnite lead isotope analyses from deposits in northern Portugal

Deposits	Location	$^{206}Pb/^{204}Pb$	$^{207}Pb/^{204}Pb$	$^{208}Pb/^{204}Pb$	$^{238}U/^{204}Pb$ μ_2	t_2 (U)	$^{232}Th/^{204}Pb$ W_2	t_2 (Th/U)
	Bragança district							
Sb	Moinho do Picão	18.188	15.608	38.425	9.77	346	39.19	112
Pb-Sb	Sítio da Coitadinha	18.216	15.623	38.270	9.83	355	38.44	197
Pb-Sb	Sítio da Coitadinha	18.254	15.667	38.417	10.02	414	39.89	117
	Dúrico-Beirão region							
Sb-Au	Abelheira	18.158	15.610	38.249	9.78	372	38.50	208
Sb-Au	Medas	18.399	15.681	38.539	10.04	335	38.63	50
Sb-Au	Borralhal	18.353	15.621	38.351	9.78	248	37.77	153
Sb-Au	Borralhal	18.520	15.620	38.133	9.74	120	35.14	271
Sb-Au	Pinheirinhos	18.278	15.589	38.211	9.66	239	36.94	229
Sb-Au	Alto do Sobrido	18.174	15.633	38.256	9.89	406	38.91	204
Sb-Au	Alto do Sobrido	18.206	15.606	38.378	9.76	328	38.74	138

Table 6
Selected antimony, lead-antimony and gold deposits from Europe

District	Location	Main type of ore	Host rock	Age of mineralization reference	Ore minerals with isotopic Pb data	Source of Pb
Brioude-Massiac, French Massif Central	Haut-Allier	Sb quartz veins, Pb-Sb quartz veins	Orthogneiss, paragneiss, schist anatexis	Permian 200-250 Ma Marcoux and Bril (1986)	Fuloppite, zinkenite, boulangerite, jameso-nite, bournonite, galena	Metamorphic basement; also granite for Pb-Sb veins
Borderies, French Massif Central	Puy de Dôme	Polymetallic veins (Sb, Pb, Zn, Ag, Cu)	Micaschist, orthogneiss	Carboniferous 313 ± 5 Ma Marcoux et al. (1988)	Berthierite, jamesonite I, II, andorite, zinkenite I, II, semseyite, plagionite	Metamorphic basement; also granites for the last stages
Pontvieux-Labessette French Massif Central	Puy de Dôme	Au-bearing quartz veins	Orthogneiss	Namurian-Westphalian (~ 320 Ma) Marcoux et al. (1985)	Jamesonite, galena, boulangerite, bournonite, senseyite	Granites and metamorphic environment
Rheinisches Schiefergebirge, Germany	Ramsbeck, Apollo, Bockstall, Caspari, Passauf, Reichen-teinerberg, Saarsegen, Silbersand, Spes	Sb quartz veins; (Cu)-Pb-Sb sulfosalt assemblages in overprinted preexisting Pb-Zn veins	Pelitic-psammitic sedimentary rocks	late-Variscan Wagner and Schneider (2002)	Bournonite, semseyite, boulangerite, stibnite, zinkenite, plagionite	Palaezoic sedimentary sequences
Lima, Central Peru	Surco	Polymetallic veins (Pb, Cu, Mo, Zn, Zb, Au)	Skarn	Undetermined Mukasa et al. (1990)	Chalcopyrite	Enriched mantle and supracrustal sediments
Cuzco, Southern Peru	Huachoc, Pucará, Agripina	Au-bearing quartz veins	Gabbro; granodiorite, volcaniclastics; diorite, tonalite	Undetermined Mukasa et al. (1990)	Chalcopyrite, pyrite, pyrite	Enriched mantle and supracrustal materials
Putina, Southern Peru	San Isidro deposit	Sb-W veins (Sn, W, Cu, Pb, Zn, Ag, Sb)	Black metapelites	Probable mid-Tertiary age (Kontak et al., 1990)	Stibnite	Involvement of radiogenic sialic crust
Baia Mare, Romania	Suior, Baia Sprie Cavnic, Herja, Sasar, Ilba Ghezuri	Au-polymetallic veins (Cu, Zn, Pb, Sb, W, Au, Ag)	Calc-alkaline volcanic rocks	Miocene (Marcoux et al., 2002)	Galena, jamesonite	Calc-alkaline volcanic activity with a mantle source and crustal assimilation

Monte Ollasteddu, Southern Sardinia, Italy	Ollasteddu, Baccu Locci, Baccherutta and Buddidorgiu	Au-Sb quartz veins	Metarhyolites and metasilstones	Post-dates Variscan basement (Dini et al., 2005)	Galena, arsenopyrite, K-feldspar	Ordovician metarhyo-lites and late-Variscan granites

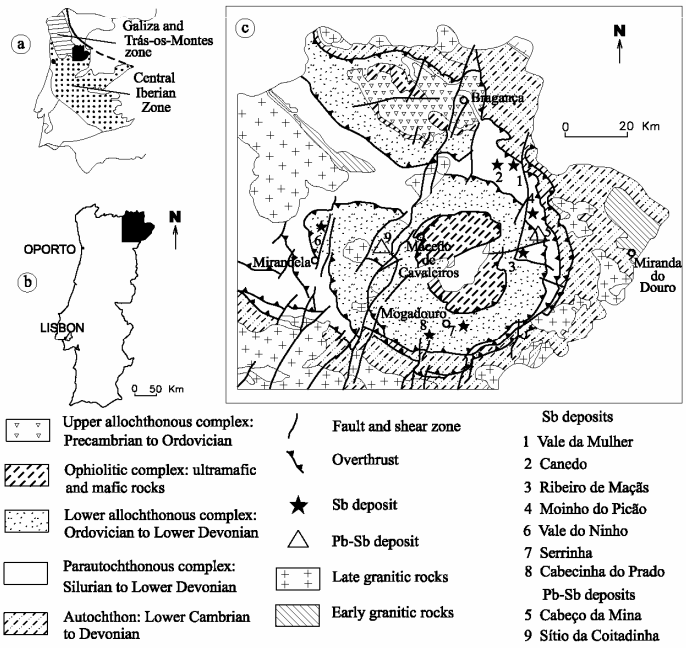

Fig 1

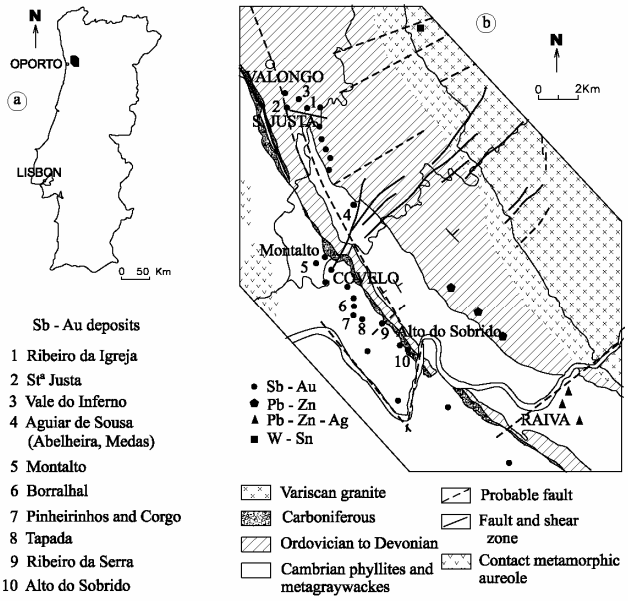

Fig 2

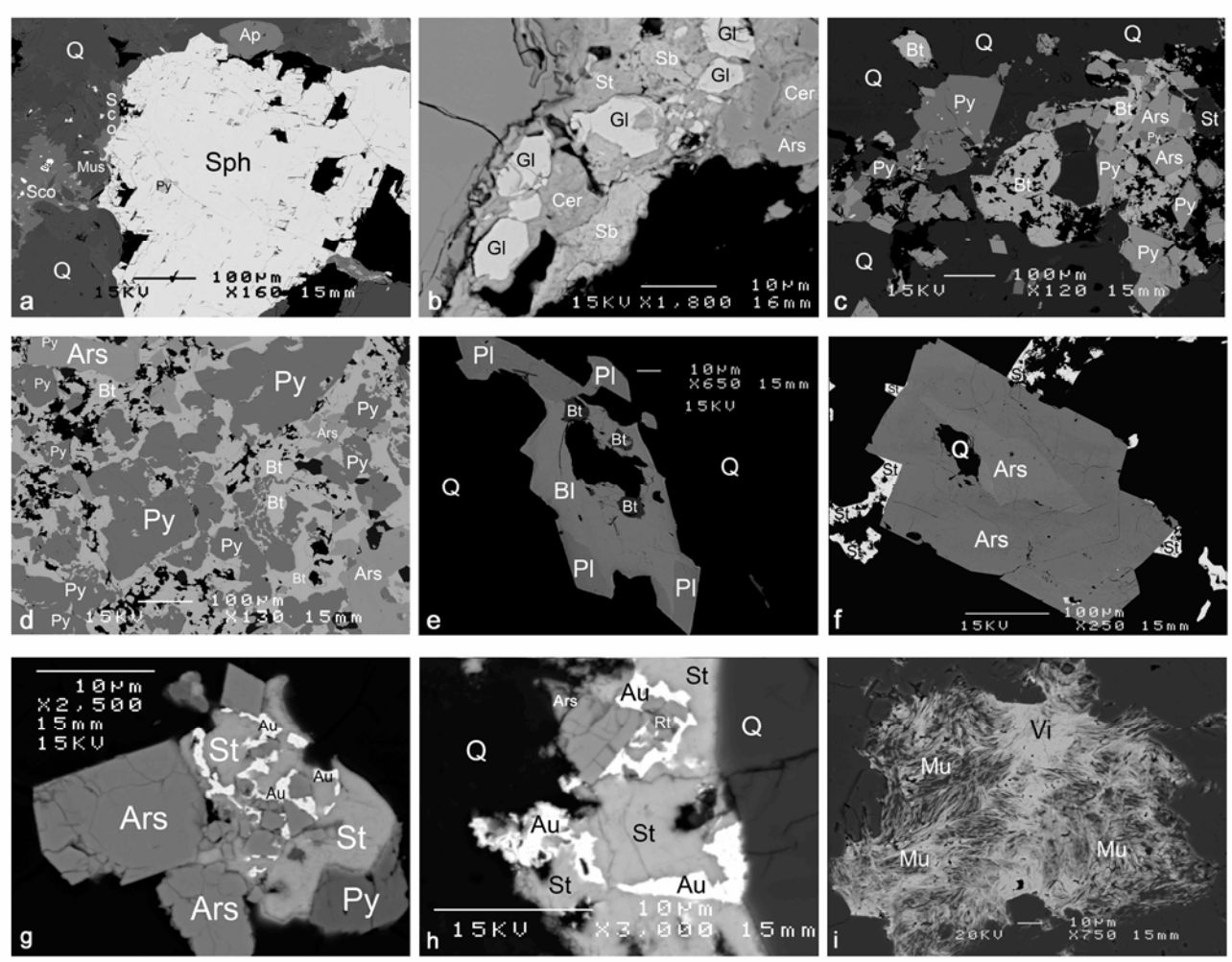

Fig 3

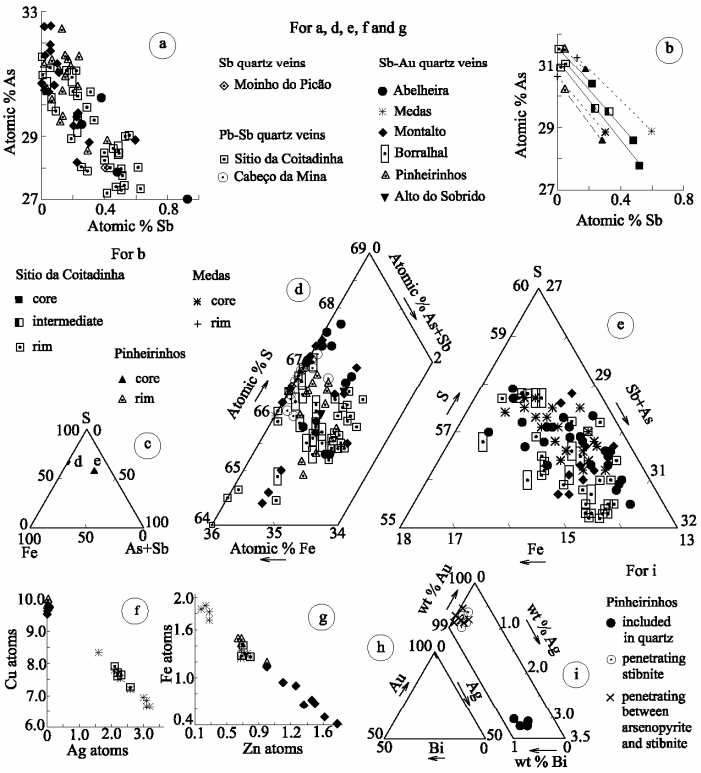

Fig 4

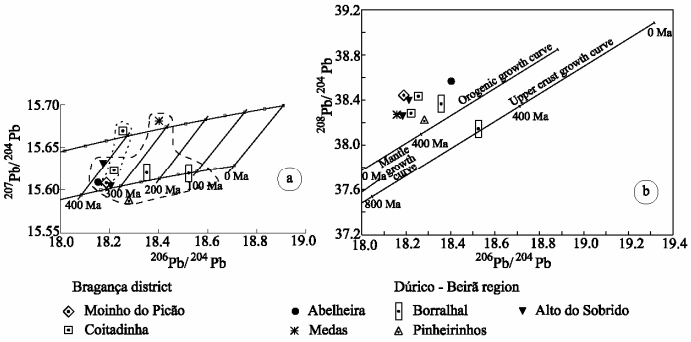

Fig 5

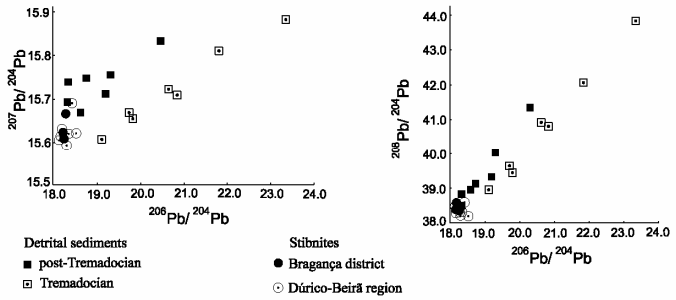

Fig 6

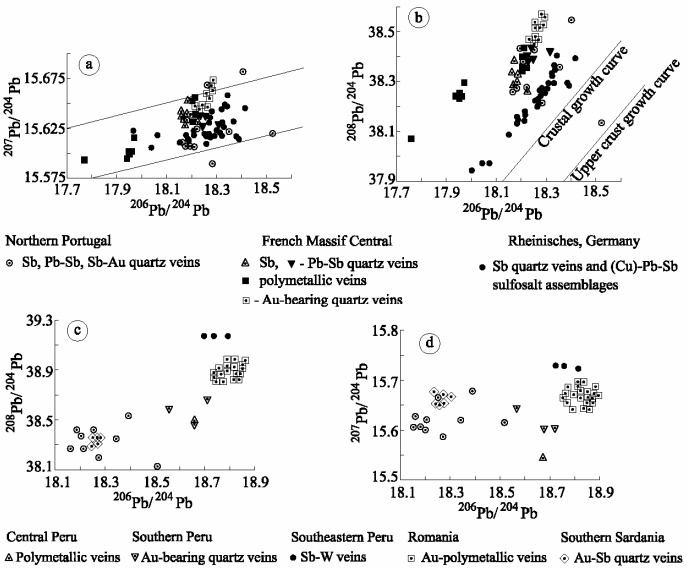

Fig 7